

Effects of sea ice change on the Arctic climate: insights from experiments with a polar atmospheric regional climate model

Xiying Liu and Chenchen Lu

ABSTRACT

To get insights into the effects of sea ice change on the Arctic climate, a polar atmospheric regional climate model was used to perform two groups of numerical experiments with prescribed sea ice cover of typical mild and severe sea ice. In experiments within the same group, the lateral boundary conditions and initial values were kept the same. The prescribed sea ice concentration (SIC) and other fields for the lower boundary conditions were changed every six hours. 10-year integration was completed, and monthly mean results were saved for analysis in each experiment. It is shown that the changes in annual mean surface air temperature have close connections with that in SIC, and the maximum change of temperature surpasses 15 K. The effects of SIC changes on 850 hPa air temperature is also evident, with more significant changes in the group with reduced sea ice. The higher the height, the weaker the response in air temperature to SIC change. The annual mean SIC change creates the pattern of differences in annual mean sea level pressure. The degree of significance in pressure change is modulated by atmospheric stratification stability. In response to reduction/increase of sea ice, the intensity of polar vortex weakens/strengthens.

Key words | Arctic climate, numerical experiment, regional climate model, sea ice

Xiying Liu (corresponding author)
College of Oceanography,
Hohai University,
Nanjing 210098,
China
E-mail: xyliu@hhu.edu.cn

Chenchen Lu
College of Meteorology and Oceanography,
National University of Defense Technology,
Changsha 410008,
China

HIGHLIGHTS

- The magnitude and extent of the Arctic climate change attributed to sea ice have been studied with a regional Arctic atmospheric model.
- Different from previous studies, the numerical experiments were conducted in pair scenarios. In this way, the robustness of response signals can be censored.
- Our results show that the consistent signals of atmospheric response to sea ice change can reach up to 500 hPa at least.

INTRODUCTION

Arctic surface air temperature (SAT) is an indicator of regional and global climate change. It has been rising at a rate of more than double the global average. The rapid

Arctic climate changes are having far-reaching impacts on natural and human systems (Boeke & Taylor 2018). Loss of sea ice and snow cover contributes to the polar amplification. There has been a decline of area covered by sea ice, snow and glaciers compared to the quantities averaged over the period from 1979 to 2005. Through various feedbacks in the climate system, these changes can enhance global warming to a greater extent (Yumashev *et al.* 2019).

This is an Open Access article distributed under the terms of the Creative Commons Attribution Licence (CC BY-NC-ND 4.0), which permits copying and redistribution for non-commercial purposes with no derivatives, provided the original work is properly cited (<http://creativecommons.org/licenses/by-nc-nd/4.0/>).

doi: 10.2166/wcc.2021.206

Under the background of global warming, both the sea ice concentration (SIC) and the duration of sea ice coverage experience rapid change (Lang *et al.* 2017). Through its unique physical characteristics compared to seawater, sea ice has an important impact on the exchange of mass, momentum, and energy between the atmosphere and the ocean (Meier *et al.* 2014). Due to that the change in SIC has a greater impact on the energy fluxes of ocean surface than that in sea surface temperature (SST) in partially sea ice covered region, it is expected that the changes of sea ice have significant influences on the evolution of atmosphere. There have been many works on understanding of the relationship between Arctic sea ice anomalies and atmospheric circulation through analyzing reanalysis datasets (e.g., Slonosky *et al.* 1997; Sorokina *et al.* 2016).

Besides analyzing reanalysis or observation datasets, numerical modeling is also widely used in the studies since numerical models are a mathematical summary of our current understanding of the real system. However, due to the limitation of computer resources, the resolution of numerical models cannot be improved limitlessly. Numerical modeling is always a tradeoff between affordable computational cost and precision requirement. Compared to global models, regional models can obtain higher resolution results. In addition, in regional polar atmospheric models, the winds that pass through the North Pole can be depicted better through adoption of suitable map projections. However, to date, work on the Arctic climate modeling with regional models are few and not systematic. In climate modeling, the setting of lower boundary in a numerical model is crucial to the overall results. Through making simulation runs at various lower boundary configurations, the effect of sea ice on the atmosphere can be investigated. From numerical experiments using the regional climate model REMO with sea ice cover diagnosed from the prescribed SST and SIC derived from satellite data respectively, Semmler *et al.* (2004) found that the introduction of partial SIC ameliorated the gradients between ice-covered and ice-free regions, which could influence precipitation and cloud cover in the Fram Strait region. Rinke *et al.* (2006) investigated the impact of forcing from the ocean on the mean atmospheric state with the regional atmospheric general circulation model RCM HIRHAM. They found that the sensitivity of SAT response to the changes of sea ice

varied seasonally. With the polar atmospheric regional climate model WRF/PCE, Liu & Xia (2014) studied the impact of changes in the lower boundary conditions (states of land surface, sea surface, and sea ice from a typical mild ice year and a severe ice year were used) on the simulated Arctic climate. It was found that, the changes in annual mean SAT were closely associated with those in underlying surface. However, the individual effect of sea ice on the atmospheric state was not isolated in their experiments. Using an atmospheric general circulation model which allows combination of a prescribed sea ice cover and an active mixed layer ocean, Pedersen *et al.* (2016) studied the atmospheric sensitivity to the location of sea ice loss. Their three scenarios with ice loss in different regions all exhibited substantial near-surface warming, which peaks over the area of ice loss.

The range of proposed mechanism involving the role of sea ice has led to some debate over the details of the relationship between the atmospheric pattern of anomaly and sea ice cover. By isolating the impact of the individual drivers in an Earth system model, Olonscheck *et al.* (2019) demonstrated that internal variability of sea ice was primarily caused directly by atmospheric temperature fluctuations. So, there is space left for further studies on the role of sea ice in the Arctic climate change. The main objective of this work is to provide insights into the effects of individual sea ice change on the Arctic climate through numerical experiments with a polar atmospheric regional climate model. The dataset used, choice of years for typical mild and severe sea ice, the employed model and design of numerical experiments are given in Methods. Results are analyzed under Results: the effects on temperature, sea level pressure, and geopotential height in 3.1–3.3 respectively. Discussion is discussion and Section 5 presents conclusions.

METHODS

Typical extent of Arctic sea ice cover for the mild and severe sea ice year was used as the lower boundary condition for the climate model and numerical experiments were performed to study the impact of sea ice change on the Arctic climate.

Dataset

The reanalysis dataset ERA-interim from ECMWF (European Centre for Medium-Range Weather Forecasts) was used for the initial value and boundary conditions of atmospheric model. SIC, SST, SAT, surface air pressure, and atmospheric variables such as wind, geopotential height, temperature and humidity at multiple pressure levels were used. These variables are in $1.5^\circ \times 1.5^\circ$ longitude-latitude grids. The initial soil and ground temperatures were also from the ERA-interim dataset.

Choice of the mild and severe sea ice year

The extent of Arctic sea ice cover is experiencing decrease in the last 20 years. In the summer of 2007, the Arctic sea ice cover had the second lowest extent in the satellite record. 2007 was chosen as the typical mild sea ice year and 1998 the typical severe sea ice year. Compared to 2007, there is more sea ice in the Chukchi Sea (CS), ESS, Laptev Sea (LS), KS, and BaS in 1998 (see Figure 1). The biggest difference is in the BaS where the SIC difference may reach up to 50%. There are areas in the ESS, LS, and KS with difference greater than 30%. From Figure 1, it can be seen that in part of the Beaufort Sea (BeS) and Greenland Sea (GS) the annual mean SIC increases weakly in 2007 compared to that in 1998.

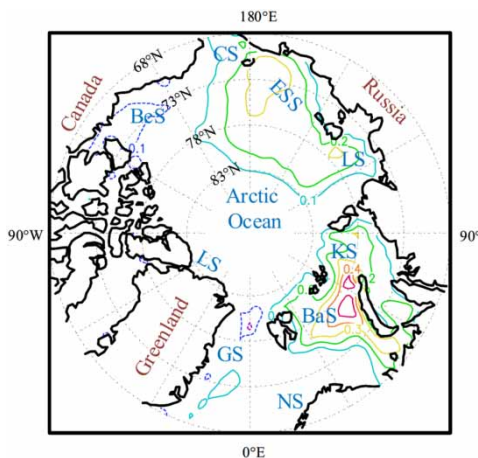


Figure 1 | Difference of annual mean SIC between 1998 and 2007. Contour interval is $0.1 \times 100\%$ with 0% not plotted. Meaning of abbreviations: GS is Greenland Sea, NS is Norway Sea, BaS is Barrents Sea, KS is Kara Sea, LS is Laptev Sea, ESS is East Siberian Sea, CS is Chukchi Sea, BeS is Beaufort Sea, and LS is Lincoln Sea.

Regional model and design of experiments

The regional climate model WRF/PCE (Polar Climate Extension version of WRF (Weather Research and Forecasting)) was used to study the effects of sea ice change on the Arctic climate. WRF/PCE was developed from NCAR (National Center for Atmospheric Research) ARW (Advance Research WRF, version 3). It inherits all ARW functions for numerical weather prediction (NWP) (Liu & Xia 2014). WRF is a state-of-the-art mesoscale model system developed for both scientific research and operational NWP needs (Skamarock *et al.* 2008). To meet the needs for application in climate studies, some modifications had been introduced into the WRF/PCE (Liu 2014).

With major model parameters as shown in Table 1, four numerical experiments were made. The configuration of model parameters was determined by the results of combination experiments involving parameterization schemes of different physical processes. This is to ensure its suitability for simulating the regional Arctic climate (Liu & Xia 2014). Differences among the experiments are the lower boundary condition in SIC and lateral boundary condition (LBC) in atmospheric state. The SIC and LBC for 2007 were used in E2007; the SIC and LBC for 1998 were used in E1998; the SIC for 1998 and LBC for 2007 were used in E2007_1998ci; the SIC for 2007 and LBC for 1998 were used in E1998_2007ci (see Table 2).

A coordinate on the stereographic projection plane was used and the center of model domain was set at the North Pole. The model used square grids with a size 50 km in the horizontal. There were 84 and 96 grids in the x and y directions respectively, and the model atmosphere was

Table 1 | Major model parameters used in the experiments

Parameters	Value
Microphysics	WSM 3-class scheme
Long wave radiation	RRTM scheme
Solar radiation	MM5 scheme
Radiation time-step	30 minutes
Surface layer	Scheme based on similarity theory
Land/water surface	PXLSSM scheme
PBL physics	Yonsei University (YSU) scheme
Cumulus parameterization	New Kain-Fritsch scheme

Table 2 | Numerical experiments

Name		Initial condition	Lower boundary of sea ice	Lateral boundary
Group (a)	E2007	2007	2007	2007
	E2007_1998ci	2007	1998	2007
Group (b)	E1998	1998	1998	1998
	E1998_2007ci	1998	2007	1998

divided into 27 layers vertically. Time step was set to 180 s in the integrations. In the experiments, the lower and lateral boundary conditions were updated every six hours, resetting to the start of the year when the current year ended. In all experiments the model was integrated for 10 years with boundary conditions looping 10 times for the year 1998 or 2007. The month-averaged model variables were saved, and the 10-year means were used to analyze the impact of sea ice cover on the climate. The land surface temperature and ground temperature were calculated by the module of land surface process.

RESULTS

Four climatological annual means of 10-year integration were obtained from the experiments. The simulations fell into 2

groups. For Group (a), comprising E2007 and E2007_1998ci, the sea ice cover was changed from a mild sea ice year to a severe one. For Group (b), comprising E1998 and E1998_2007ci, the sea ice cover was changed from a severe sea ice year to a mild one. The amplitude of sea ice change in both groups were identical. But due to the differences in other fields between the two groups, the response of atmosphere to sea ice change may be different. This will help deepening the understanding of uncertainties in modeling the effects of sea ice change on the atmosphere. To confirm the reliability of the results, the differences between numerical experiments were subjected to a Student's t-test, with a significance level of $\alpha = 0.05$. The analysis had been focused on the impact of sea ice on the atmosphere in temperature, sea level pressure, and geopotential height.

Temperature

Sea ice anomalies influence the atmosphere through exerting direct local thermal forcing. This will be reflected in air temperature, especially SAT obviously. Changes in SAT between E2007 and E2007_1998ci are shown in Figure 2(a). When sea ice is severe in E2007_1998ci, the SAT over most of the domain decreased. The contour centers of SAT difference coincide with that of SIC differences well (compare

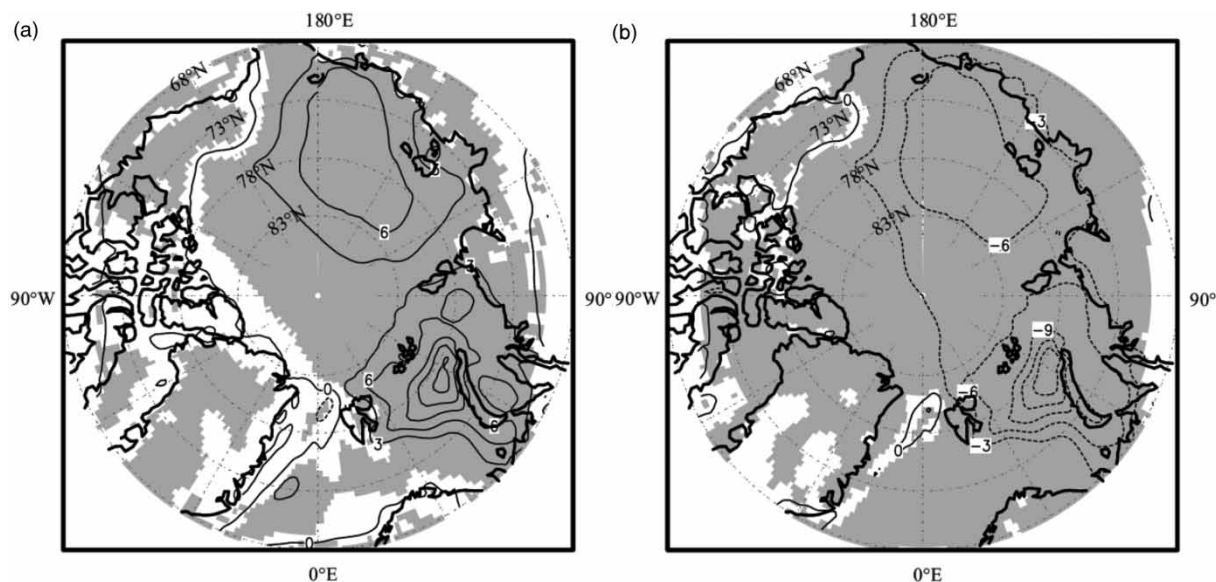


Figure 2 | Difference of SAT (a) between E2007 and E2007_1998ci and (b) between E1998 and E1998_2007ci. Contour interval is 3 °C and areas passed t-test with $\alpha = 0.05$ are shaded.

Figure 2(a) with Figure 1). Major centers are in the ESS and BaS. In the ESS, the maximum difference is more than 6 K. In the BaS, the maximum difference is more than 15 K. There are temperature increases in part of the BeS and GS, which corresponds to a reduction of sea ice in those regions. Associated with SIC difference in the KS, there are also two regions with relatively larger SAT difference.

The pattern of changes in SAT between E1998 and E1998_2007ci is similar to that between E2007 and E2007_1998ci (compare Figure 2(a) with Figure 2(b)) except that the signs of SAT difference are opposite due to the reverse SIC change. The geographical extent of SAT difference with magnitude greater than 3 K in Group (a) (between E2007 and E2007_1998ci) is different from that in Group (b) (between E1998 and E1998_2007ci). This reflects the modulation of other factors such as differences in land surface characteristics, sea surface temperature, and lateral boundary conditions. From the simulation results (Figure 2), it is clear that the SAT differences are dominated by the effect of sea ice change.

At 850 hPa, the warming/cooling due to reduced/increased sea ice has been spread over a wider area, and the position of warming center in Figure 3(a) is not coincident with that of the cooling center in Figure 3(b). The warming center deduced from temperature difference

between E2007 and E2007_1998ci is in the Arctic Ocean. Whereas the cooling center deduced from temperature difference between E1998 and E1998_2007ci is in the BaS. This implies that, at higher levels, the role of other processes such as advection and internal variability in determining the temperature variation strengthens. At 500 hPa, the impact of sea ice change on air temperature is further reduced. At 200 hPa, there is no discernable significant difference in temperature (figures not shown).

From the simulation results, it is shown that the changes in sea ice lead to atmospheric warming/cooling through a direct local surface heating/cooling over the sea ice anomaly region. Over regions without big sea ice anomaly, an indirect atmospheric warming/cooling is also visible. The major indirect effect is the advection process which redistributes the temperature at higher levels. The ultimate feature of air temperature distribution involves the coupling between the surface and free atmosphere through the planetary boundary layer (PBL).

SLP

SLP reflects the total air mass over the seas. The warmer/colder air column are associated with reduced/increased SLP. Since the air density is greater at lower levels and the

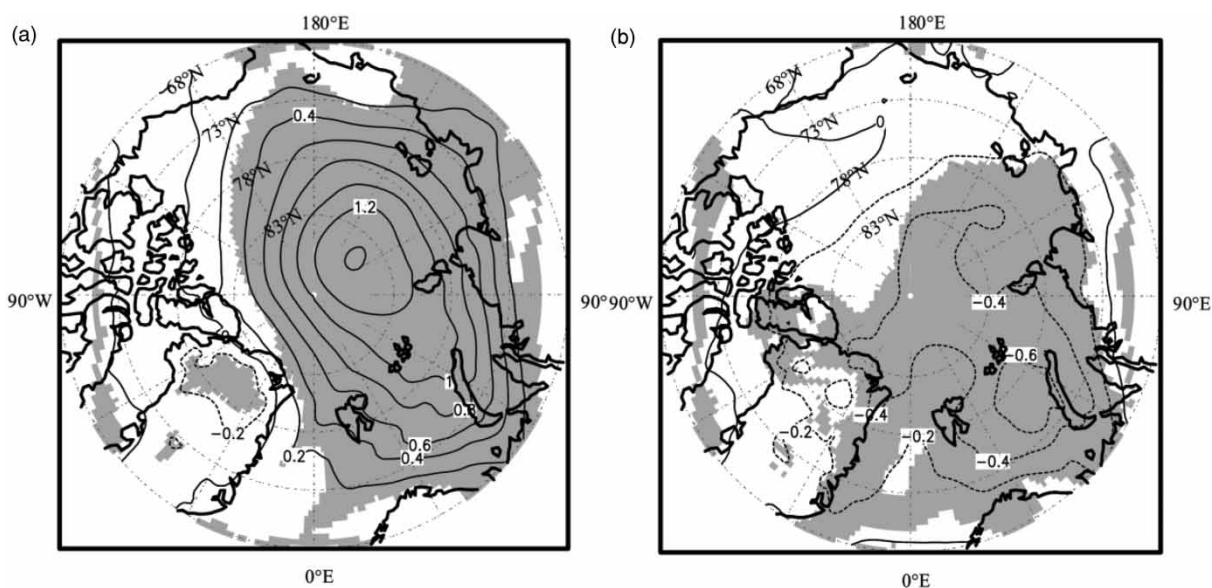


Figure 3 | Difference of air temperature at 850 hPa (a) between E2007 and E2007_1998ci and (b) between E1998 and E1998_2007ci. Contour interval is 0.2 °C and areas passed t-test with $\alpha = 0.05$ are shaded.

total air mass over the seas is largely influenced by the low-level atmosphere, colder/warmer SAT most likely coincides with an increased/decreased mean SLP. Associated with the distribution of SIC anomalies, there are anomalies in SLP over the ESS, KS, and BaS (Figure 4). Through exerting a local thermal forcing to the atmosphere, the SIC anomalies give rise to the SAT anomalies in the ESS, KS, and BaS, which in turn induces the SLP changes in those regions (see Figures 1, 2 and 4). The maximum SLP change is about 3 hPa. This is consistent with results of numerical experiments from other studies (for example, Rinke *et al.* 2006; Liu & Xia 2014). From Figure 4, it is seen that the pattern of significance for SLP difference between the two groups are different. The SLP differences in the ESS and LS pass the statistical significance test in results from group a. However, it does not in results from group b. In addition, the area passing the statistical test in the BaS and KS from group a is larger than that from group b. The differences in magnitude of the effect of sea ice change on SLP between the two groups are due to the influence of atmospheric stratification stability. In case of sea ice reduction, SAT increases and the air is less stable. This helps warming the upper air and decreasing the SLP. In case of sea ice increase, SAT decreases and the air is more stable. This inhibits cooling the upper air effectively and increasing the SLP.

Geopotential height

The change of air temperature forced by sea ice anomalies modifies the variation of geopotential height locally under the constraint of static equilibrium. However, the variation of geopotential height is also influenced by other processes, such as geostrophic adjustment and transient wave activities. The simulated impacts of sea ice changes on geopotential height at 850 hPa and 500 hPa are shown in Figures 5 and 6. At both levels, the differences in geopotential height over the Arctic Ocean from group a are not statistically significant. Whereas the differences in geopotential height over the BaS and KS from group b pass the statistical significance test. The centers of difference contours in geopotential height at 500 hPa from both groups are close to the North Pole, implying a weakening/strengthening of the polar vortex intensity, in response to reduction/increase of sea ice, respectively. The pattern of change in geopotential height at 200 hPa is similar to that at 500 hPa in group a but quite different from that at 500 hPa in group b (Figure S1 in the Supplementary Material). The maximum change of geopotential height at 500 hPa is about 10 gpm (geopotential meter, an adjustment to geometric height (elevation above mean sea level) using the variation of gravity with latitude and elevation. 1 gpm

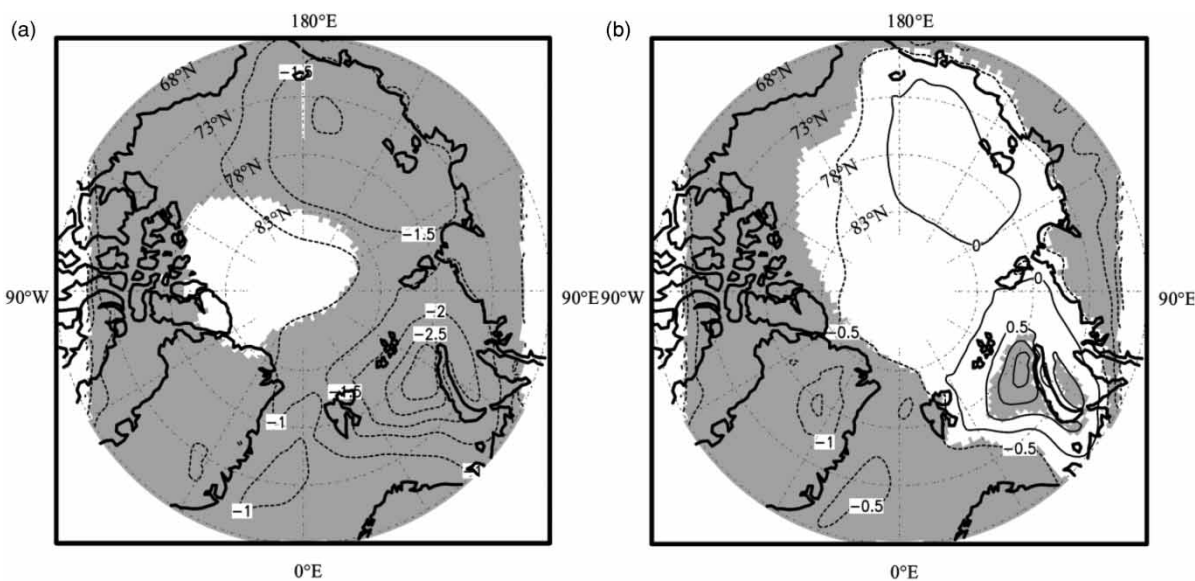


Figure 4 | Difference of sea level pressure (a) between E2007 and E2007_1998ci and (b) between E1998 and E1998_2007ci. Contour interval is 0.5 hPa and areas passed t-test with $\alpha = 0.05$ are shaded.

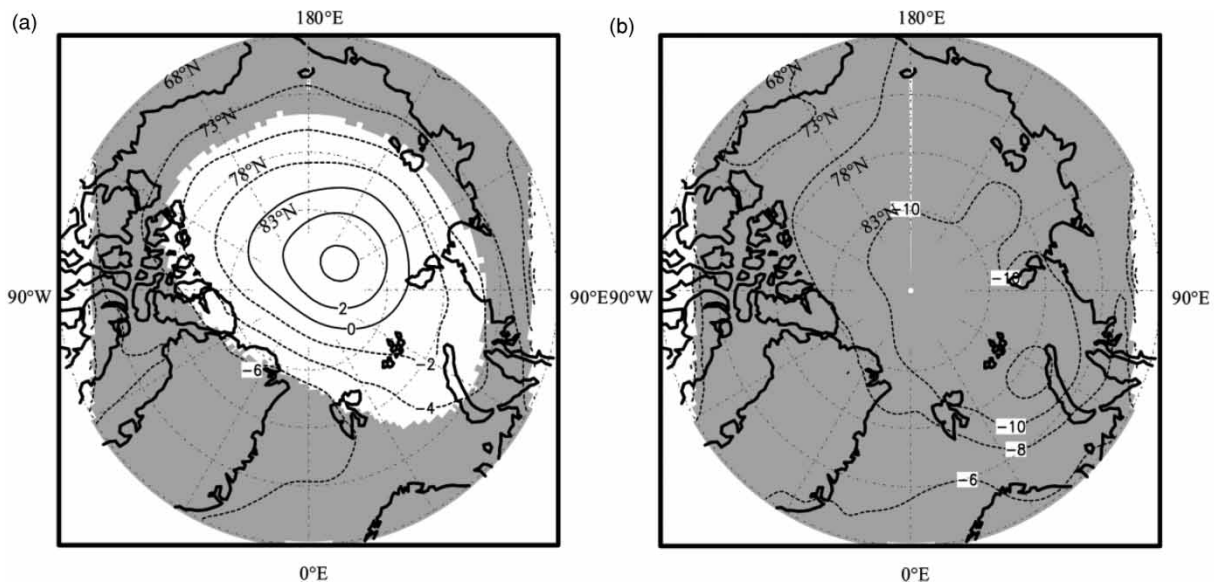


Figure 5 | Difference of geopotential height at 850 hPa (a) between E2007 and E2007_1998ci and (b) between E1998 and E1998_2007ci. Contour interval is 2 gpm and areas passed t-test with $\alpha = 0.05$ are shaded.

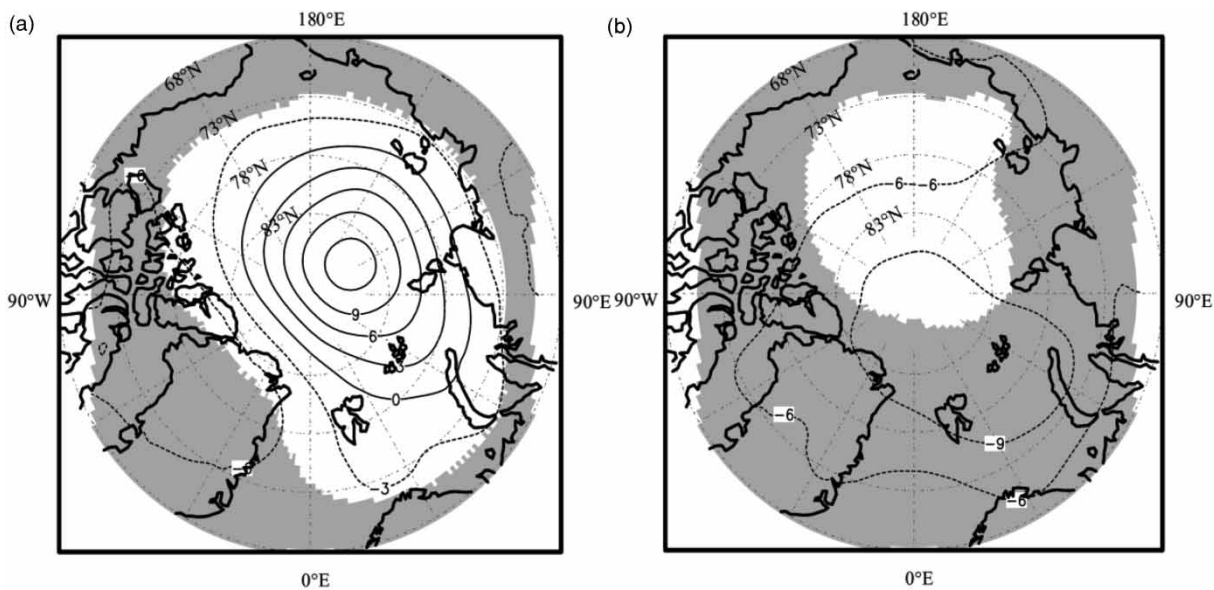


Figure 6 | Difference of geopotential height at 500 hPa (a) between E2007 and E2007_1998ci and (b) between E1998 and E1998_2007ci. Contour interval is 3 gpm and areas passed t-test with $\alpha = 0.05$ are shaded.

is equal to 1 m on the mean sea level), which is of the same order as in the experiments of Rinke *et al.* (2006) and Liu & Xia (2014). From Figures 5 and 6, it is shown that the response to sea ice change in geopotential height is quasi-barotropic. This is consistent with earlier results from numerical simulation (e.g., Rinke *et al.* 2006).

DISCUSSION

In the previous section, we studied the impact of sea ice change on the Arctic climate through prescribing sea ice cover in numerical experiments with a regional atmospheric model. In the study, the experiments in each group have

identical boundary conditions, and the domain of simulation is not large. This ensures that the internal variability is not strong and the differences in simulated climate are mainly controlled by the forcing of differences in sea ice cover. Through isolating the individual effect of sea ice cover on the polar climate, the causal chain of climate change is clear. Sea ice extent in the summer of 2007 is the second smallest in the history of satellite observation. Sea ice extent in the summer of 2020 is the third smallest. Since the decadal trend of sea ice decrease remains, the sea ice scenario of 2007 may be close to the mean state of the future decade. The results from E2007 can shed light on the climate in a sense of decadal mean in the near future. The goal was to explore the magnitude and extent of the Arctic climate response to sea ice cover change. Our results show that the consistent signals of atmospheric response to sea ice change can reach up to 500 hPa at least. Different from previous studies, the experiments were conducted in pair scenarios (group (a) and group (b)). In this way, the robustness of response signals was censored and the influence of other factors from the difference in atmospheric initial state could be detected.

In reality, the Arctic climate involves complicated interactions between the ocean and the atmosphere. The uncoupled atmospheric climate model cannot reflect such interactions and does not account for the driving of atmosphere on surface ocean variability (Sorokina *et al.* 2016). Without mechanism of feedback, biases may be enlarged in simulation results from the uncoupled model. Fluxes from ocean to atmosphere can be unrealistically strong and persistent in the uncoupled model and the internal atmospheric variability may be reduced (Barsugli & Battisti 1998). In addition, to evaluate the uncertainties due to difference in models, more work with different atmospheric models are needed.

The impact of sea ice cover changes in the Arctic on the climate may be more extensive in geography. The study of its global effects is beyond the scope of the current work.

CONCLUSION

In the work, the impact of sea ice on the Arctic climate had been investigated through numerical experiments in the

context of sea ice change from a typical severe/mild year to a typical mild/severe year. The aim of the research was to evaluate the extent to which the sea ice cover affect the Arctic climate simulated by a polar atmospheric regional climate model and to derive implications for uncertainties in the Arctic climate simulation. It was clear that the changes of sea ice had influence on the simulated Arctic climate. The main conclusions are:

The impact of changes in sea ice cover on SAT is significant, and the largest difference is greater than 15 K. Typical characteristics of a thermal response are also exhibited in air temperature at 850 hPa with wider area compared to that at ocean surface. As atmospheric height increases, the impact of the SIC change on temperature decreases. At higher levels, other processes such as advection and internal variability play more role in determining the temperature variation.

Through exerting thermal forcing to the local air, the SIC anomalies give rise to the SAT anomalies in the ESS, KS, and BaS, which in turn induces SLP changes in those regions. The maximum SLP change is about 3 hPa. The pattern of SLP differences coincides with that of major annual mean SIC change. The significance of SLP differences is modulated by stratification stability near the sea surface.

The SIC change causes differences in the geopotential height at both 850 and 500 hPa. The major contour centers of geopotential height difference at 500 hPa in both groups are near the North Pole, implying changes in polar vortex strength.

ACKNOWLEDGEMENTS

This work is partly supported by the Fundamental Research Funds for the Central Universities in China (2019B00214). The ERA-Interim datasets were downloaded from <https://apps.ecmwf.int/datasets/data/interim-full-daily/>. The Student's t-tests were calculated with function `OneSampleTTest` of `StatsKit` package in Julia.

DATA AVAILABILITY STATEMENT

Data cannot be made publicly available; readers should contact the corresponding author for details.

REFERENCES

- Barsugli, J. J. & Battisti, D. S. 1998 The basic effects of atmosphere-ocean thermal coupling on midlatitude variability. *J. Atmos. Sci.* **55**, 477–493. [https://doi.org/10.1175/1520-0469\(1998\)055<0477:TBEAOA>2.0.CO;2](https://doi.org/10.1175/1520-0469(1998)055<0477:TBEAOA>2.0.CO;2).
- Boeke, R. C. & Taylor, P. C. 2018 Seasonal energy exchange in sea ice retreat regions contributes to differences in projected Arctic warming. *Nat. Commun.* **9**, 5017. <https://doi.org/10.1038/s41467-018-07061-9>.
- Lang, A., Yang, S. & Kaas, E. 2017 Sea ice thickness and recent warming. *Geophys. Res. Lett.* **44**, 409–418. <https://doi.org/10.1002/2016GL071274>.
- Liu, X. 2014 Biases of the Arctic climate in a regional ocean–sea ice atmosphere coupled model: an annual validation. *Acta Oceanol. Sin.* **33**, 56–67. <https://doi.org/10.1007/s13131-014-0518-2>.
- Liu, X. Y. & Xia, H. S. 2014 *Adv. Polar. Sci.* **25**, 261–268. <https://doi.org/10.13679/j.advps.2014.1.00261>.
- Meier, W., Hovelsrud, G., van Oort, B., Key, J., Kovacs, K., Michel, C., Haas, C., Granskog, M., Gerland, S., Perovich, D., Makshtas, A. & Reist, J. 2014 Arctic sea ice in transformation: a review of recent observed changes and impacts on biology and human activity. *Rev. Geophys.* **52**, 185. <https://doi.org/10.1002/2013RG000431>.
- Olonscheck, D., Mauritsen, T. & Notz, D. 2019 Arctic sea-ice variability is primarily driven by atmospheric temperature fluctuations. *Nat. Geosci.* **12**, 430–434. <https://doi.org/10.1038/s41561-019-0363-1>.
- Pedersen, R. A., Cvijanovic, I., Langen, P. L. & Vinther, B. M. 2016 The impact of regional Arctic sea ice loss on atmospheric circulation and the NAO. *J. Climate* **29**, 889–902. <https://doi.org/10.1175/JCLI-D-15-0315.1>.
- Rinke, A., Maslowski, W., Dethloff, K. & Clement, J. 2006 Influence of sea ice on the atmosphere: a study with an Arctic atmospheric regional climate model. *J. Geophys. Res.* **111**, D16103. <https://doi.org/10.1029/2005JD006957>.
- Semmler, T., Jacob, D., Schluenzen, K. H. & Podzun, R. 2004 Influence of sea ice treatment in a regional climate model on boundary layer values in the Fram Strait region. *Mon. Weather Rev.* **132**, 985–999. [https://doi.org/10.1175/1520-0493\(2004\)132<0985:IOSITI>2.0.CO;2](https://doi.org/10.1175/1520-0493(2004)132<0985:IOSITI>2.0.CO;2).
- Skamarock, W. C., Klemp, J. B., Dudhia, J., Gill, D. O., Barker, B. M., Duda, M. G., Huang, X. Y., Wang, W. & Powers, J. G. 2008 *A Description of the Advanced Research WRF Version 3*. NCAR Technical Note, National Center for Atmospheric Research, Boulder. Available from: https://www.researchgate.net/publication/306154004_A_Description_of_the_Advanced_Research_WRF_Version_3 (accessed 6 March 2020)
- Slonosky, V. C., Mysak, L. A. & Derome, J. 1997 Linking Arctic sea-ice and atmospheric circulation anomalies on interannual and decadal timescales. *Atmosphere-Ocean*. **35**, 333–366.
- Sorokina, S. A., Li, C., Wettstein, J. J. & Kvamstø, N. G. 2016 Observed atmospheric coupling between Barents Sea ice and the warm-Arctic cold-Siberian anomaly pattern. *J. Climate* **29**, 495–511. <https://doi.org/10.1175/JCLI-D-15-0046.1>.
- Yumashev, D., Hope, C., Schaefer, K., Riemann-Campe, K., Iglesias-Suarez, F., Jafarov, E., Burke, E. J., Young, P. J., Elshorbany, Y. & Whiteman, G. 2019 Climate policy implications of nonlinear decline of Arctic land permafrost and other cryosphere elements. *Nat. Commun.* **10**, 1900. <https://doi.org/10.1038/s41467-019-09863-x>.

First received 4 July 2020; accepted in revised form 30 October 2020. Available online 25 March 2021